

## Impact of 2-deoxy-D-glucose on the target metabolome profile of a human endometrial cancer cell line

Kenichi URAKAMI<sup>1</sup>, Vincent ZANGIACOMI<sup>2</sup>, Ken YAMAGUCHI<sup>2</sup>, and Masatoshi KUSUHARA<sup>2</sup>

<sup>1</sup>Cancer Diagnostics Division and <sup>2</sup>Regional Resources Division, Shizuoka Cancer Center Research Institute, 1007 Shimonagakubo, Nagaizumi-cho, Sunto-gun, Shizuoka 411-8777, Japan

(Received 12 July 2013; and accepted 6 August 2013)

### ABSTRACT

2-deoxy-D-glucose (2DG) has been clinically evaluated for its potential use as an anticancer drug. Although 2DG is generally thought to inhibit the glycolytic pathway through accumulation of 2-deoxy-D-glucose-6-phosphate (2DG6P), it may also interfere with various other biological processes. Here, to further understand the role of 2DG as an inhibitor of tumor progression, we assessed the metabolism of 2DG in a human endometrial cancer cell line using capillary electrophoresis-time-of-flight mass spectrometry (CE-TOFMS). A total of 113 target metabolite peaks were identified and 90 metabolites of them were quantified. Furthermore, we present a new methodology which uses CE-TOFMS metabolome profiling following introduction of an artificial metabolite to evaluate tumor-specific metabolite traces. Aside from 2DG6P, we detected the presence of unique 2DG-derived deoxy metabolites in 2DG-treated cells. These metabolites may be responsible for the alteration of global metabolism in cells and act as various biological effectors.

Enhanced aerobic glycolysis is a metabolic hallmark of cancer, and inhibiting this process in cancer cells is generally considered a promising therapeutic strategy for halting disease progression (14, 24, 30). While most normal cells acquire energy through pyruvate oxidation in the mitochondria, cancer cells do so predominantly through glycolysis followed by lactic acid production in the cytosol, even in the presence of sufficient oxygen (31, 32). One small molecule which has been found to interfere with cancer-specific metabolic pathways is 2-deoxy-D-glucose (2DG). This molecule is currently under evaluation as a potential drug in either single or combination chemotherapy (5, 33).

Although 2DG is primarily considered to inhibit the glycolytic pathway, it may also interfere with other biological processes. 2DG is characterized as

a non-metabolized glucose analogue which has the 2-hydroxyl group replaced by hydrogen. It is also known to be phosphorylated by hexokinase to form 2-deoxy-D-glucose-6-phosphate (2DG6P), which cannot be further metabolized but rather accumulates in the cell, where it blocks glycolysis and thereby leads to the depletion of cellular ATP and subsequent cell death (4, 27). In a recent study, prostate cancer cells treated with a combination of metformin and 2DG showed the significant cell death associated with decrease in cellular ATP (2). Metformin is a well-established diabetes drug that inhibits the function of complex I in the mitochondrial electron transport chain leading to the depletion of cellular ATP. 2DG also decrease cellular ATP through the inhibition of the glycolysis. The depletion of the two main sources of ATP leads to a drastic reduction in cellular ATP levels.

Enhanced glycolysis has therefore been assessed for cancer diagnosis in the clinical field by using 2-([<sup>18</sup>F]fluoro)-2-deoxy-D-glucose (2FDG) as a radiotracer in PET-CT imaging. 2FDG contains a radioactive fluorine in place of the hydroxyl group at the C-2 position in the glucose molecule, which pre-

---

Address correspondence to: Masatoshi Kusuhara, MD  
Regional Resources Division, Shizuoka Cancer Center  
Hospital and Research Institute, 1007 Shimonagakubo,  
Nagaizumi-cho, Sunto-gun, Shizuoka 411-8777, Japan  
Tel: +81-55-989-5222 (Ext. 6043), Fax: +81-55-989-6085  
E-mail: m.kusuhara@sccchr.jp

vents its further metabolization in the cell (10). Malignant cells can be identified as those showing higher 2FDG uptake under PET-CT imaging.

Here, to better understand the role of 2DG as an inhibitor of tumor progression, we used capillary electrophoresis-time-of-flight mass spectrometry (CE-TOFMS) to evaluate the effect of 2DG on the metabolome profile in a human endometrial cancer cell line. Endometrial cancer is the most common gynecologic malignancy in the United States and accounts for 5.8% of all cancers in women (9). Although the reported incidence in Japan is eight times less than that in the United States and Canada, prevalence has nevertheless increased rapidly over the last 10 years (29). Treatment options for endometrial cancer remain limited, however, suggesting the need for further investigation of potential therapeutic targets. Despite its potential as an anticancer drug, the effect of 2DG in endometrial cancer cell lines has yet to be investigated.

The HEC-1-A cell line, established in 1968, was the first to be derived from a human endometrial carcinoma, and the first from a human adenocarcinoma of any organ except HeLa cells. HEC-1-A cells have been used in various studies aimed at evaluating the characteristics of human endometrial carcinoma (15).

One means of better understanding the overall effect of 2DG metabolism in cancer cells might be CE-TOFMS, which has recently been recognized as a powerful tool for the comprehensive investigation of metabolic processes (22, 25, 26). Here, we used CE-TOFMS to investigate tumor-specific metabolite traces in the HEC-1-A cell line following exposure to 2DG.

## MATERIALS AND METHODS

**Cell culture.** The human endometrial cancer cell line HEC-1-A (ATCC No. HTB-112) was purchased from the American Type Culture Collection (Manassas, VA, USA). Cells were subcultured in 75-cm<sup>2</sup> tissue culture flasks (Corning Glass Works, Corning, NY, USA) and maintained in DMEM (Gibco, Life Technologies, Carlsbad, CA, USA) supplemented with 10% fetal bovine serum and 50 mg/mL gentamycin (Gibco, Life Technologies) at 37°C in water-saturated air with 5% CO<sub>2</sub>.

**Sample collection for metabolite extraction.** Cells were seeded into 10-cm<sup>2</sup> culture dishes and incubated under standard growth conditions until 80% confluence was reached. Culture medium with 6 mM

2DG (Sigma-Aldrich, St. Louis, MO, USA) or culture medium only was added to each dish and removed after 8 h. The cells were then quickly washed twice with ice-cold 5% maltose-water solution, and residual 5% maltose-water solution was removed by vacuum. The cells were then quenched using 1 mL LC-MS grade methanol (Sigma-Aldrich), and gently detached from the culture dish using a cell scraper (MS-93170; Sumitomo Chemical, Tokyo, Japan). The methanol solution containing the quenched cells was transferred to a 10 mL centrifuge tube for extraction. Additional cells were cultured in the same manner and the number of cells was counted for normalization of metabolite concentrations. Intracellular metabolites were extracted using two-phase liquid extraction. Methanol, chloroform, and water were mixed in a 10 : 10 : 4 volume ratio. The aqueous phase contained water-soluble endogenous low-molecular-weight metabolites; the organic phase contained non-polar metabolites, such as lipids; and the solvent layer between the two phases contained macromolecules, such as proteins. The aqueous phase was collected for extraction of water-soluble endogenous low-molecular-weight metabolites and centrifugally filtered through a 5-kDa cut-off filter (Millipore, Billerica, MA, USA) to remove macromolecules. The solvent was completely removed using a vacuum concentrator (Thermo Electron, Waltham, MA, USA), and the residue was dissolved in 50 µL Milli-Q water containing internal standards and immediately subjected to CE-TOFMS analysis.

**Analytic conditions for metabolome analysis.** All CE-TOFMS experiments were performed using the Agilent Capillary Electrophoresis (CE) System equipped with an Agilent 6224 TOFMS, Agilent 1200 isocratic HPLC pump, Agilent G1603 CE-MS adapter kit, and Agilent G1607 CE-electrospray ionization (ESI)-MS sprayer kit (Agilent Technologies, Santa Clara, CA, USA). For system control and data acquisition, the G2201AA ChemStation software was used for CE and MassHunter software for TOFMS (Agilent Technologies). Cationic and anionic metabolite analysis was performed with the HMT Metabolomics Solution Package (Human Metabolome Technologies Inc., Yamagata, Japan) according to the published method (20, 21, 28). Briefly, standard compounds (a kind gift from Human Metabolome Technologies, Inc.) were analyzed as references for *m/z* values, migration times and quantification. Standard compounds were: glycolic acid, lactic acid, fumaric acid, 2-oxoisovaleric acid, succinic acid, malic acid, phosphoenolpyruvic acid, dihydroxyace-

tone phosphate, glycerol-3-phosphate, cis-aconitic acid, 3-phosphoglyceric acid, citric acid, isocitric acid, gluconic acid, ribose 5-phosphate, ribulose 5-phosphate, fructose 6-phosphate, glucose 6-phosphate, glucose 1-phosphate, 6-phosphogluconic acid, sedoheptulose 7-phosphate, dTMP, CMP, cAMP, fructose 1,6-diphosphate, cGMP, AMP, IMP, GMP, PRPP, dTDP, CDP, acetylCoA, ADP, GDP, dCTP, dTTP, CTP, UTP, dATP, ATP, GTP, NAD<sup>+</sup>, NADP<sup>+</sup>, Gly, putrescine,  $\beta$ -Ala, Ala,  $\gamma$ -aminobutyric acid, Ser, cytosine, uracil, creatinine, Pro, Val, homoserine, Thr, Cys, hydroxyproline, creatine, Ile, Leu, Asn, ornithine, Asp, adenine, hypoxanthine, anthranilic acid, tyramine, spermidine, Gln, Lys, Glu, Met, guanine, His, Phe, Arg, citrulline, Tyr, DOPA, spermine, Trp, carnosine, cytidine, uridine, adenosine, inosine, guanosine, glutathione (GSSG) divalent, glutathione (GSH) and S-adenosylmethionine. Reference MS spectra for 20 compounds from HMT Metabolome database library were used for annotation. The twenty compounds were: uric acid, dRMP, glucosamine 6-phosphate, N-acetyl D-glucosamine 6-phosphate, deoxycytidine 3-monophosphate, dUMP, UMP, dAMP, UDP, dADP, dGDP, dGTP, UDP-glucose, xanthine, D-glucono-1,5-lactone, D-glucosamine, N-acetyl D-glucosamine, 2'-deoxycytidine, thymidine, and 2'-deoxyadenosine. 2-deoxy-D-glucose-6-phosphate was purchased from Sigma-Aldrich as standard compound. Raw data containing thousands of peaks were processed using the MasterHands software (Keio University) for quantification of metabolites. This software has been used in several previous CE-TOFMS-based profiling studies (7, 18). The overall data processing flow was as follows: migration time alignment, peak detection, background subtraction, and integration of peak area from a 0.02 *m/z*-wide slice of the electropherogram. All target metabolites were identified by comparing their *m/z* values and migration times to those of the standard compounds. A total of 93 compounds were annotated and quantified. For each sample, the measured metabolite concentrations were normalized by cell number to obtain the amount of metabolite contained per million cells (nmol/M cells).

**Data visualization.** Data were visualized using the open source program VANTED (Visualization and Analysis of Networks Containing Experimental Data, <http://vanted.ipk-gatersleben.de/>), which allows the mapping of potential biological pathways (13).

## RESULTS AND DISCUSSION

In this study, we assessed the effect of 2DG on the metabolome profile in a human endometrial cancer cell line. A total of 113 target metabolites were identified and 90 metabolites of them were quantified by comparing their *m/z* values and migration times to those of standard compounds using CE-TOFMS.

Our observations were consistent with the role of 2DG6P as a competitive inhibitor of phosphoglucose isomerase, which converts glucose 6-phosphate (G6P) to fructose 6-phosphate (F6P) (1), and as a noncompetitive inhibitor of hexokinase, which phosphorylates glucose to G6P (19). The level of G6P, the first metabolite of the glycolytic pathway, was 4.0-fold higher in 2DG-treated than untreated cells (Fig. 1). Further, F6P was almost completely absent in 2DG-treated cells (Fig. 1). In addition, levels of glycolytic metabolites downstream of F6P, including fructose 1,6-diphosphate, dihydroxyacetone phosphate, 3-phosphoglyceric acid and phosphoenolpyruvic acid, were several-fold lower in treated cells (Fig. 1). The accumulated G6P in treated cells probably shunted glucose to the pentose phosphate pathway (PPP). Consistent with this, concentrations of PPP metabolites, namely 6-phosphogluconic acid, ribulose 5-phosphate (Ru5P), ribose 5-phosphate (Rb5P), sedoheptulose 7-phosphate, and erythrose 4-phosphate, were 3.9-, 3.2-, 3.8-, 2.8- and 2.0-fold higher, respectively, in 2DG-treated than untreated cells (Fig. 2). With regard to glycogen synthesis, G1P, the first metabolite, was almost undetected as a result of accumulation of 2DG6P, which may be a competitive inhibitor of phosphoglucomutase (Fig. 1).

Although 2DG is generally thought to induce the accumulation of 2DG6P, and thereby inhibit the glycolytic pathway, the present study showed that 2DG may alter global metabolism and interfere with various other biological processes. Our results showed that despite this block in the glycolytic pathway, ATP level was only moderately higher in 2DG-treated than untreated cells (Fig. 3). Additionally, metabolites levels in the TCA cycle, which produces ATP, did not markedly differ between treated and untreated cells (Fig. 1), further suggesting that 2DG may interfere not only with glucose metabolism, but also with that of other biological processes as well.

Concentrations of ornithine, S-adenosylmethionine, and putrescine, which are related to the polyamine pathway, also differed between 2DG-treated and untreated cells (Fig. 1). In particular, ornithine levels were higher and putrescine levels lower in

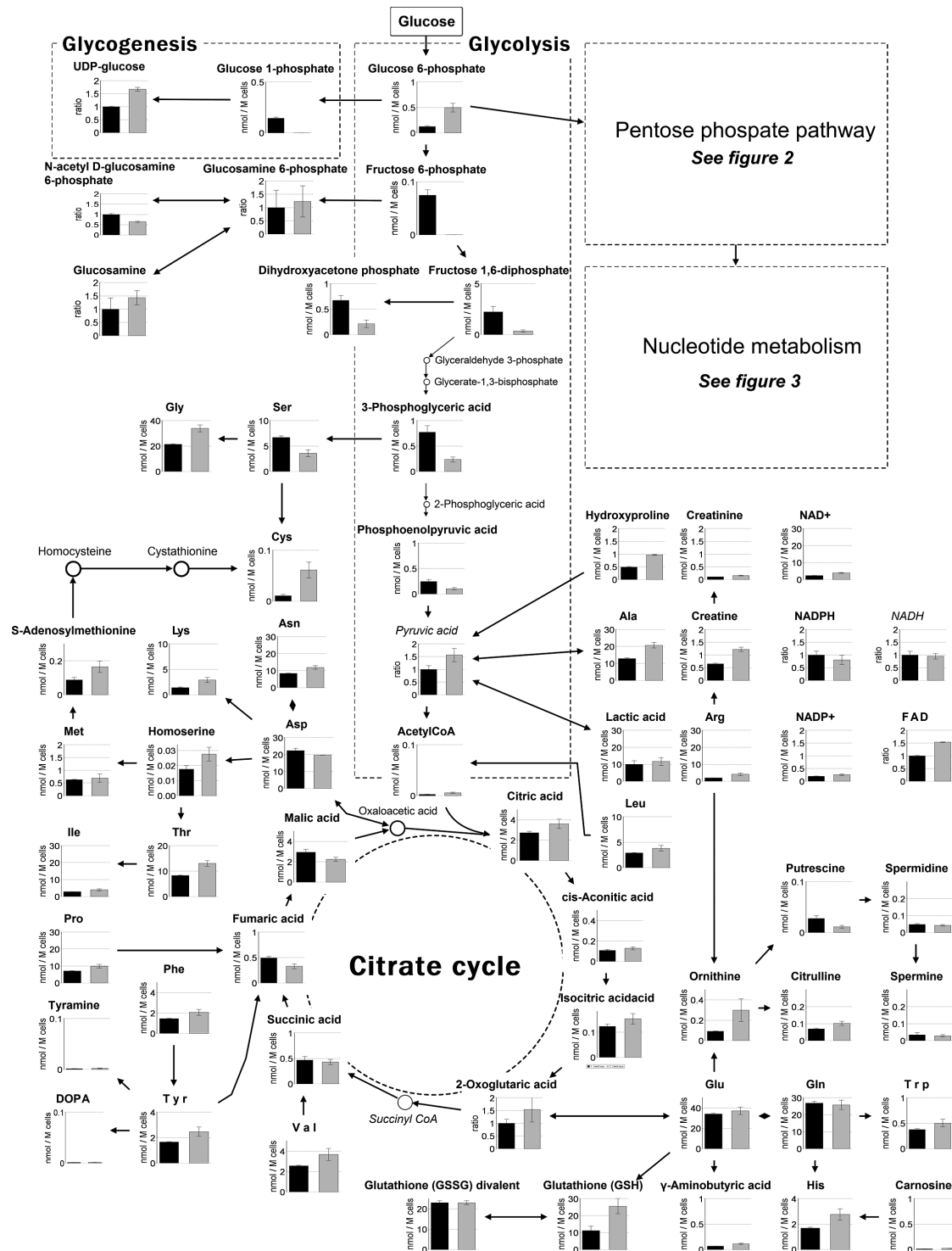


**Fig. 1** Pathway map of metabolites in glycogenesis, glycolysis, the citrate cycle and amino acids in 2DG-treated and -untreated cells. Grey and black boxes represent metabolite concentrations (nmol/million cells) in 2DG-treated and -untreated cells, respectively. Italicized metabolites were not quantified due to a lack of standard compounds, and represent the concentration ratio relative to the control. All error bars represent the S.D. ( $n = 3$ ). The level of glucose 6-phosphate was 4.0-fold higher in 2DG-treated than -untreated cells. Further, fructose 6-phosphate was almost completely absent in 2DG-treated cells. In addition, levels of glycolytic metabolites downstream of F6P, including fructose 1,6-diphosphate, dihydroxyacetone phosphate, 3-phosphoglyceric acid and phosphoenolpyruvic acid, were several-fold lower in treated cells. The accumulated G6P in treated cells probably shunted glucose to the pentose phosphate pathway (PPP).

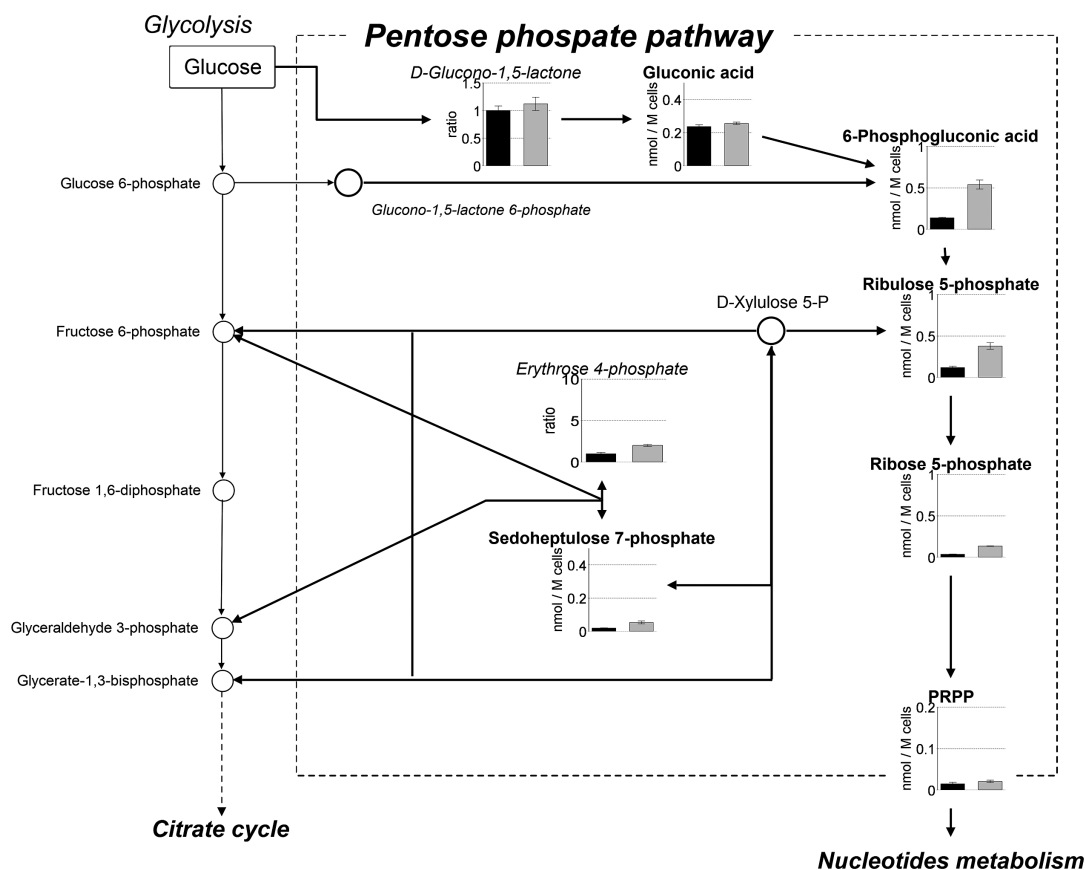


**Fig. 2** Pathway map of metabolites in the pentose phosphate pathway in 2DG-treated and -untreated cells. Grey and black boxes represent metabolite concentrations (nmol/Million cells) in 2DG-treated and -untreated cells, respectively. Italicized metabolites were not quantified due to a lack of standard compounds, and represent the concentration ratio relative to the control. All error bars represent the S.D. ( $n = 3$ ). 6-Phosphogluconic acid, ribulose 5-phosphate (Ru5P), ribose 5-phosphate (Rb5P), sedoheptulose 7-phosphate, and erythrose 4-phosphate, were several fold higher, respectively, in 2DG-treated than -untreated cells. With regard to glycogen synthesis, G1P, the first metabolite, was almost undetected as a result of accumulation of 2DG6P, which may be a competitive inhibitor of phosphoglucomutase.

2DG-treated cells. This may reflect the decreased activity of ornithine decarboxylase, which decarboxylates ornithine to putresine. One study reported that cysteine strongly inhibits the activity of ornithine decarboxylase (3). Cysteine levels in 2DG-treated cells is in fact quite high (Fig. 1). The cysteine is provided via glyceraldehyde 3-phosphate, which is likely derived from the pentose phosphate pathway rather than the glycolysis pathway.

Several other studies suggest that incorporation of 2DG may affect various biological pathways. For instance, one study reported that the anticancer properties of 2DG correlate with changes in the N-linked glycosylation pattern in the target tissue (16). In that study, 2DG was found to alter N-linked glycosylation, leading to protein unfolding and disruption of thiol metabolism, thereby causing oxidative stress.

We speculated that if 2DG metabolites aside from 2DG6P were early intermediates of other biological pathways, peaks corresponding to these 2DG metabolites would be detected by CE-TOFMS with retention times similar to those of the original compounds in 2DG-treated cells only. The peaks corresponding to deoxy analogs were detected by subtracting 15.994 (the exact mass of oxygen) from the  $m/z$  value of the original 113 metabolites. In fact, 20 Mass peaks considered to correspond to the original compounds appeared at high concentrations in 2DG-treated cells only. While the retention times of some of these metabolites differed markedly from those of the original compounds, retention times of the nine metabolites were notably close to those of the correspondents. Based on this observation, we speculated that peaks which were at nearly the same retention time as the correspondents must be those of 2-deoxy

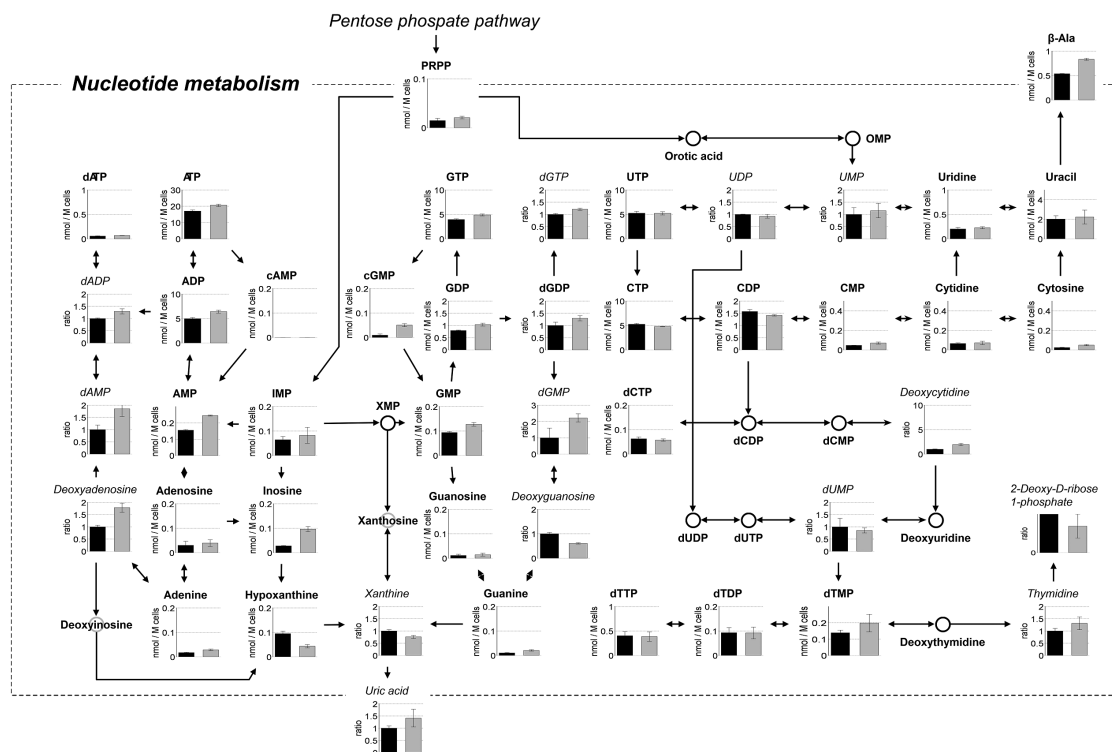


**Fig. 3** Pathway map of metabolites in nucleotide metabolism in 2DG-treated and -untreated cells. Grey and black boxes represent metabolite concentrations (nmol/million cells) in 2DG-treated and -untreated cells, respectively. Italized metabolites were not quantified due to a lack of standard compounds, and represent the concentration ratio relative to the control. All error bars represent the S.D. ( $n = 3$ ). ATP level was only moderately higher in 2DG-treated than -untreated cells.

metabolites. In particular, the 2DG6P peak was found to be at a markedly high area peak value of over 1000 (Fig. 4). For reference, area peak values for G6P in treated and untreated cells were 10.1 and 2.7 respectively. All original peaks that were in treated cells were also present in untreated cells. Additional 2-deoxy-metabolites, namely 2-deoxy-analogues of 6PGA, gluconic acid and Rb6P for PPP, and 2-deoxy-analogues of G1P and UDP-glucose for glycogen synthesis, were detected (Fig. 4). Migration times of the original and 2-deoxy metabolites were 13.22 min and 13.29 min, 7.52 min and 7.48 min, 9.96 min and 10.22 min, 9.24 min and 9.66 min, and 7.93 min and 7.98 min, respectively.

Due to enzyme specificity and substrate structure, 2-deoxy-G6P-derived metabolites are unlikely to exist in the cell. Nevertheless, two studies using  $F^{18}$ -NMR examining the metabolism of 2FDG, an analog of 2DG, have reported the existence of 2-deoxy-2-fluoro-D-mannose (FDM), FDG-6-phosphate, UDP-FDM, and GDP-FDM as unique metabolites downstream of FDG-6-phosphate (11, 12).

The competitive level of 2-deoxy-UDP-glucose, which is a critical intermediate substrate of (Glu)<sub>3</sub>

(Man)<sub>7</sub>(GlcNAc)<sub>2</sub>-dolichyl diphosphate in N-glycan biosynthesis, was detected in 2DG-treated cells. Integration of UDP-2-deoxy-glucose or guanine diphosphate 2-deoxy-mannose (or both) into (Glu)<sub>3</sub>(Man)<sub>7</sub>(GlcNAc)<sub>2</sub>-dolichyl diphosphate may therefore result in various biological malfunctions, and may also induce changes in the expression and phosphorylation status of proteins involved in signaling, cell cycle control, DNA repair, calcium influx, and apoptosis (6, 8). Furthermore, a recent genome-wide analysis identified 19 2DG-resistant yeast knockouts lacking genes implicated in carbohydrate metabolism and mitochondrial homeostasis, as well as ribosome biogenesis, mRNA decay, transcriptional regulation, and cell cycle control (23).

In this study we demonstrated that the advantages of CE-MS analysis include its extremely high resolution, high throughput, and ability to simultaneously quantify all charged low-molecular-weight compounds in a sample. For each sample, the measured metabolite concentrations were presented as the level of nmol/million cells, as shown in Fig 1. These metabolites were all charged, low-molecular-weight compounds and separated within an analysis time

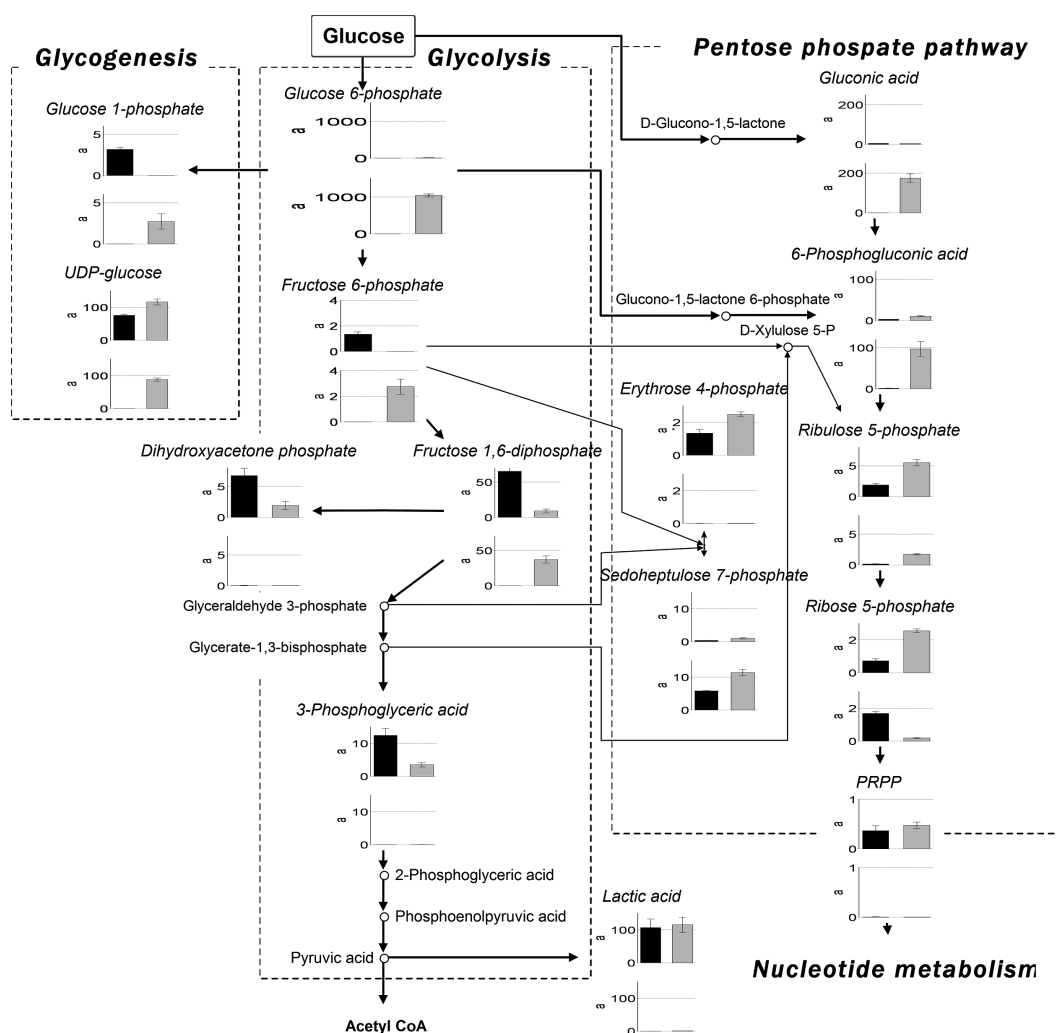


**Fig. 4** Pathway map of original and deoxy metabolites in 2DG-treated and untreated cells. Grey and black boxes represent metabolite quantity (area peak value mass spectrometry) in 2DG-treated and -untreated cells, respectively. Metabolite quantities in the lower charts are 15.9949 (exact mass of oxygen) less than corresponding values in the upper charts. All error bars represent the S.D. ( $n = 3$ ). Area peak for 2DG6P (lower chart in Glucose-6-phosphate) was found to be at a markedly high value of over 1000. For reference, area peak for G6P (upper chart in Glucose-6-phosphate) in treated and untreated cells were 10.1 and 2.7 respectively. Additional 2-deoxy-metabolites, namely 2-deoxy-analogues of 6-Phosphogluconic acid, gluconic acid and Ribulose 5-phosphate for PPP, and 2-deoxy-analogues of G1P and UDP-glucose for glycogen synthesis, were detected (lower chart).

of 40 min. Compounds having the same molecular weight and similar chemical properties, such as G6P, F6P and G1P, cannot be separated by liquid or gas chromatography. These metabolites can, however, be successfully distinguished and quantified by capillary electrophoresis coupled with mass spectrometry. We therefore found CE-TOFMS to be a precise and powerful tool for comprehensive metabolome profiling which provided novel information about 2DG metabolome profiling in cultured cancer cells.

Several limitations of this study warrant mention. First, precise identification of some metabolites was

difficult because of a lack of corresponding standard compounds. Second, the characteristics of capillary electrophoresis meant that only hydrophilic metabolites were exclusively detected. Third, snapshot-like data at a single time point cannot grasp information arising from metabolic flux.

Results showed that 2DG is likely to alter global metabolism via the effects of 2DG-derived metabolites. To our knowledge, this is the first study to examine whether the use of metabolome profiling through CE-TOFMS after introduction of an artificial metabolite can be used to evaluate tumor-specific

ic metabolite traces.

Similar to the way in which testing glucose tolerance is a diagnostic tool in diabetic patients, tumor-specific metabolite profiling of blood for tolerance to artificial and original metabolites may be a new diagnostic tool in cancer patients. Our findings highlight the importance of verifying the antitumor effect of 2DG from a metabolic point of view. Further studies of the biological mechanisms by which 2DG metabolites affect cell viability, such as by inducing apoptosis or blocking the cell cycle (or both), may have important therapeutic implications in cancer.

### Acknowledgements

This study was supported by Regional Innovation Cluster Program from the Ministry of Education, Culture, Sports, Science and Technology-Japan.

### REFERENCES

- Achari A, Marshall SE, Muirhead H, Palmieri RH and Noltmann EA (1981) Glucose-6-phosphate isomerase. *Philos Trans R Soc Lond B Biol Sci* **293**, 145–157.
- Ben Sahra I, Laurent K, Giuliano S, Larbret F, Ponzio G, Gounon P, Le Marchand-Brustel Y, Giorgetti-Peraldi S, Cormont M, Bertolotto C, Deckert M, Auberger P, Tanti JF and Bost F (2010) Targeting cancer cell metabolism: the combination of metformin and 2-deoxyglucose induces p53-dependent apoptosis in prostate cancer cells. *Cancer Res* **70**, 2465–2475.
- Chabanon H, Persson L, Wallace HM, Ferrara M and Brachet P (2000) Increased translation efficiency and antizyme-dependent stabilization of ornithine decarboxylase in amino acid-supplemented human colon adenocarcinoma cells, Caco-2. *Biochem J* **348**, 401–408.
- Demetrakopoulos GE, Linn B and Amos H (1982) Starvation, deoxy-sugars, ouabain, and ATP metabolism in normal and malignant cells. *Cancer Biochem Biophys* **6**, 65–74.
- Dwarakanath BS, Singh D, Banerji AK, Sarin R, Venkataramana NK, Jalali R, Vishwanath PN, Mohanti BK, Tripathi RP, Kalia VK and Jain V (2009) Clinical studies for improving radiotherapy with 2-deoxy-D-glucose: present status and future prospects. *J Cancer Res Ther* **5**, S21–S26.
- Heminger K, Jain V, Kadakia M, Dwarakanath B and Berberich SJ (2006) Altered gene expression induced by ionizing radiation and glycolytic inhibitor 2-deoxy-glucose in a human glioma cell line: implications for radio sensitization. *Cancer Biol Ther* **5**, 815–823.
- Hirayama A, Kami K, Sugimoto M, Sugawara M, Toki N, Onozuka H, Kinoshita T, Saito N, Ochiai A, Tomita M, Esumi H and Soga T (2009) Quantitative metabolome profiling of colon and stomach cancer microenvironment by capillary electrophoresis time-of-flight mass spectrometry. *Cancer Res* **69**, 4918–4925.
- Hunter AJ and Blekkenhorst GH (1998) The effects of 2-deoxyglucose and amino-oxyacetic acid on the radiation response of mammalian cells in vitro. *Int J Radiat Biol* **73**, 311–324.
- Jemal A, Siegel R, Ward E, Hao Y, Xu J, Murray T and Thun MJ (2008) Cancer statistics, 2008. *CA Cancer J Clin* **58**, 71–96.
- Jones SC, Alavi A, Christman D, Montanez I, Wolf AP and Reivich M (1982) The radiation dosimetry of 2-[F-18]fluoro-2-deoxy-D-glucose in man. *J Nucl Med* **23**, 613–617.
- Kanazawa Y, Yamane H, Shinohara S, Kuribayashi S, Momozono Y, Yamato Y, Kojima M and Masuda K (1996) 2-Deoxy-2-fluoro-D-glucose as a functional probe for NMR: the unique metabolism beyond its 6-phosphate. *J Neurochem* **66**, 2113–2120.
- Kanazawa Y, Umayahara K, Shimmura T and Yamashita T (1997) <sup>19</sup>F NMR of 2-deoxy-2-fluoro-D-glucose for tumor diagnosis in mice. An NDP-bound hexose analog as a new NMR target for imaging. *NMR Biomed* **10**, 35–41.
- Klukas C and Schreiber F (2010) Integration of -omics data and networks for biomedical research with VANTED. *J Integr Bioinform* **7**, 112–117.
- Kroemer G and Pouyssegur J (2008) Tumor cell metabolism: cancer's Achilles' heel. *Cancer Cell* **13**, 472–482.
- Kuramoto H, Hamano M and Imai M (2002) HEC-1 cells. *Hum Cell* **15**, 81–95.
- Kurtoglu M, Gao N, Shang J, Maher JC, Lehrman MA, Wangpaichitr M, Savaraj N, Lane AN and Lampidis TJ (2007) Under normoxia, 2-deoxy-D-glucose elicits cell death in select tumor types not by inhibition of glycolysis but by interfering with N-linked glycosylation. *Mol Cancer Ther* **6**, 3049–3058.
- Lin X, Zhang F, Bradbury CM, Kaushal A, Li L, Spitz DR, Aft RL and Gius D (2003) 2-Deoxy-D-glucose-induced cytotoxicity and radiosensitization in tumor cells is mediated via disruptions in thiol metabolism. *Cancer Res* **63**, 3413–3417.
- Minami Y, Kasukawa T, Kakazu Y, Iigo M, Sugimoto M, Ikeda S, Yasui A, van der Horst GT, Soga T and Ueda HR (2009) Measurement of internal body time by blood metabolomics. *Proc Natl Acad Sci USA* **106**, 9890–9895.
- Meyerhof O (1927) Ueber die enzymatische Milch-saurebildung im Muskelextrakt; die Milch-saurebildung aus den garfahigen Hexosen. *Biochem Z* **183**, 176–215.
- Ohashi Y, Hirayama A, Ishikawa T, Nakamura S, Shimizu K, Ueno Y, Tomita M and Soga T (2008) Depiction of metabolome changes in histidine-starved *Escherichia coli* by CE-TOFMS. *Mol Biosyst* **4**, 135–147.
- Ooga T, Ohashi Y, Kuramitsu S, Koyama Y, Tomita M, Soga T and Masui R (2009) Degradation of ppGpp by nudix pyrophosphatase modulates the transition of growth phase in the bacterium *Thermus thermophilus*. *J Biol Chem* **284**, 15549–15556.
- Ramautar R, Mayboroda OA, Somsen GW and de Jong GJ (2011) CE-MS for metabolomics: Developments and applications in the period 2008–2010. *Electrophoresis* **32**, 52–65.
- Ralser M, Wamelink MM, Struys EA, Joppich C, Krobitsch S, Jakobs C and Lehrach H (2008) A catabolic block does not sufficiently explain how 2-deoxy-D-glucose inhibits cell growth. *Proc Natl Acad Sci USA* **105**, 17807–17811.
- Rodríguez-Enríquez S, Marín-Hernández A, Gallardo-Pérez JC, Carreño-Fuentes L and Moreno-Sánchez R (2009) Targeting of cancer energy metabolism. *Mol Nutr Food Res* **53**, 29–48.
- Soga T, Ohashi Y, Ueno Y, Naraoka H, Tomita M and Nishioka T (2003) Quantitative metabolome analysis using capillary electrophoresis mass spectrometry. *J Proteome Res* **2**, 488–494.
- Sugimoto M, Hirayama A, Robert M, Abe S, Soga T and Tomita M (2010) Prediction of metabolite identity from ac-

- curate mass, migration time prediction and isotopic pattern information in CE-TOFMS data. *Electrophoresis* **31**, 2311–2318.
27. Thakkar NS and Potten CS (1993) Inhibition of doxorubicin-induced apoptosis in vivo by 2-deoxy-D-glucose. *Cancer Res* **53**, 2057–2060.
  28. Urakami K, Zangiacoimi V, Yamaguchi K and Kusuhara M (2010) Quantitative metabolome profiling of *Illicium anisatum* by capillary electrophoresis time-of-flight mass spectrometry. *Biomed Res* **31**, 161–163.
  29. Ushijima K (2009) Current status of gynecologic cancer in Japan. *J Gynecol Oncol* **20**, 67–71.
  30. Vander Heiden MG, Cantley LC and Thompson CB (2009) Understanding the Warburg effect: the metabolic requirements of cell proliferation. *Science* **324**, 1029–1033.
  31. Warburg O, Posener K and Negelein E (1924) Über den Stoffwechsel der Carcinomzelle. *Biochem Z* **152**, 309–344.
  32. Warburg O (1956) On the origin of cancer cells. *Science* **123**, 309–314.
  33. Zhong D, Liu X, Schafer-Hales K, Marcus AI, Khuri FR, Sun SY and Zhou W (2008) 2-Deoxyglucose induces Akt phosphorylation via a mechanism independent of LKB1/AMP-activated protein kinase signaling activation or glycolysis inhibition. *Mol Cancer Ther* **7**, 809–817.